infrastructures

MDPI

Article

Assessment of Community Risk from Seismic-Induced Damage to Hazardous Materials Storage Tanks in Marine Ports

Mohamad Nassar, Fatiha Mouri and Ahmad Abo El Ezz *

Construction Engineering Department, École de Technologie Supérieure, Université du Québec, Montreal, QC H3C 1K3, Canada; mohamad.nassar@etsmtl.ca (M.N.); fatiha.mouri.1@ens.etsmtl.ca (F.M.)
* Correspondence: ahmad.abo-el-ezz@etsmtl.ca

Abstract

Marine ports located in regions of moderate seismicity can face high Natech (natural hazard-triggered technological) risk because large inventories of hazardous materials are stored near dense urban populations. This study proposes and applies a Natech risk framework to a representative port on the Saint-Laurence River in Quebec, Canada. Site-specific peak ground accelerations (PGA) are first estimated for 12 earthquake scenarios using regional ground motion prediction equations adjusted for local site conditions. These hazard levels are combined with a damage probability matrix to estimate Hazardous Release Likelihood Index (HRLi) scores for atmospheric steel storage tanks. Offsite consequences are then evaluated to obtain Maximum Distances of Effect (MDEs) for different types of hazardous materials. MDE footprints are intersected with block-level demographic data and complemented by a domino-effect based on inter-tank spacing, yielding a tank-level Natech Risk Index $NRI_{i,s}$ for each storage tank (i) and seismic scenario (s). These values are then averaged over all tanks to obtain a scenario-level mean Natech Risk Index ($\overline{NRI}$) for each tank substance. Regression equations relating $\overline{NRI}$ to PGA are provided as a practical tool for defining critical intensity thresholds for seismic Natech risk management in marine ports.

Keywords: Natech risk assessment; marine ports; seismic risk; population exposure; storage tanks

1. Introduction

Marine ports support both global and regional energy supply chains by handling the import, export and storage of petroleum products, crude oil, liquefied petroleum gas (LPG) and other essential fuels. Situated along shorelines adjacent to major urban centers to allow efficient ship-to-shore transfers, these facilities bring high-hazard industrial installations into proximity with dense populations, creating the potential for Natech (natural hazards trigger technological accidents) events [1]. An important complementary perspective in the context of Natech risk is that of resilience, which emphasizes not only hazard assessment and vulnerability but also the capacity of infrastructure systems and communities to prepare for, withstand and recover from hazardous events. Recent work has highlighted the role of resilience frameworks in supporting risk-informed decision-making for critical infrastructure systems exposed to interacting natural and technological hazards [2]. Integrating resilience considerations with seismic Natech risk assessment can strengthen both mitigation prioritization and post-event planning by explicitly linking risk drivers to adaptive and recovery strategies.

Academic Editors: Mojtaba Harati, John W. van de Lindt and Maria Koliou

Received: 30 December 2025
Revised: 25 January 2026
Accepted: 29 January 2026
Published: 2 February 2026

Recent advances in Natech risk assessment have increasingly emphasized the need for integrated frameworks that explicitly link natural hazards, technological vulnerability, cascading effects and population exposure. Shafiei-Moghaddam et al. [3] developed a scenario-based seismic Natech framework for earthquake-induced chemical releases, demonstrating that risk escalation becomes pronounced once critical shaking thresholds are exceeded, particularly in regions where historical seismic data are limited. Their work highlights the importance of tracing the full pathway from ground motion to damage, release likelihood and off-site consequences rather than addressing these components in isolation.

Uncertainty-aware and system-level approaches have also gained prominence. For example, Kabir et al. [4] developed a Bayesian belief network-based Natech risk assessment model that explicitly propagates uncertainty across seismic hazard, equipment vulnerability and release pathways. While probabilistic methods offer valuable insights into uncertainty interactions, they often require extensive data and calibration, which may not be readily available for many port facilities. As a result, recent studies have emphasized the complementary role of scenario-based, deterministic approaches as effective screening tools for comparative risk evaluation and decision support in data-limited environments.

Earthquakes present a particular hazard in this context in two ways. The primary arises when seismic ground motions deform tank foundations, undermine anchorage systems and induce liquid sloshing and roof uplift in large storage vessels. Under earthquake shaking, storage tanks exhibit distinct failure mechanisms. Compressive hoop stresses at the shell base can trigger elephant-foot buckling once lateral displacements exceed critical levels [5]. Floating roofs face sloshing-induced uplift that can compromise roof seals and vents [6]. Tanks without anchorage may slide or overturn when inertial forces exceed frictional resistance. Furthermore, liquefaction-induced differential settlement can damage even anchored structures.

A secondary threat results from phenomena such as soil liquefaction, uneven ground settlement and surface cracking, all of which can amplify structural vulnerability. Should any containment fail under these stresses, flammable or toxic substances may escape, forming vapor clouds that can ignite, deflagrate or detonate and thus produce fires, explosions and widespread collateral damage.

Marine ports typically rest upon reclaimed sediments or alluvial deposits that often amplify seismic ground motions through complex site response. In regions of moderate seismicity, such as Eastern Canada, probabilistic seismic hazard assessments rely on regional ground motion prediction equations calibrated to local strong motion records. For example, Atkinson and Adams [7], Pezeshk et al. [8] and Pavel et al. [9] relate earthquake magnitude, source distance and average shear-wave velocity in the upper thirty m (V_{s30}) to peak ground acceleration (PGA) and spectral ordinates.

In parallel, resilience-oriented perspectives have been increasingly incorporated into Natech risk analysis. A systematic review by [10] synthesizes applications of Resilience Engineering principles to Natech accidents in the chemical and process industry, identifying key methods and gaps in how resilience is currently integrated into risk assessment frameworks. Similarly, Castro Rodríguez et al. [11] proposed a resilience-based framework for NaTech risk management in industrial critical infrastructures that emphasizes stages such as awareness, preparedness and recovery, highlighting the need to go beyond immediate consequence analysis to include adaptive and recovery capacities.

These resilience-oriented contributions underscore the value of identifying critical intensity thresholds and supporting more effective prioritization of mitigation and emergency-planning strategies tailored to complex multi-hazard environments.

In coastal regions of moderate seismicity, such as the eastern Canadian provinces, including Quebec [12], the historic earthquake record is sparse, leading to a systematic

underestimation of seismic risk [13]. Bridging this gap requires a quantitative framework that traces the entire sequence from seismic ground motion to community-level impacts. Existing assessments often address seismic hazard and technological vulnerability in isolation, rather than within an integrated, site-specific approach that explicitly captures the damage pathways linking ground shaking to hazardous-materials release and human exposure [3]. Cruz and Okada [14] established a Natech risk framework featuring a five-step workflow: geospatial inventory development, estimation of hazard release levels via damage analysis, domino effect scoring to account for cascading failures, mapping of population exposure using consequence analysis buffers and calculation of a NaTech Risk Index (NRI) by aggregating the product of release magnitude, effect distance and exposed population [15].

Subsequent studies have enhanced this workflow with high-resolution geographic information system inventories using unmanned aerial vehicle and LiDAR data, Bayesian networks to propagate uncertainty [4] and agent-based evacuation simulations to capture dynamic exposure patterns [16]. Offsite consequence analysis software such as RMP Comp [17] and ALOHA simulates vapor-cloud dispersion, pool fire thermal radiation and overpressure zones, delineating generated threat zone estimates.

The importance of cascading effects and industrial clustering has been clearly demonstrated in the recent literature. Zhou et al. [16] employed agent-based modeling to simulate Natech events in chemical clusters and showed that inter-facility interactions and escalation patterns significantly influence the timing and extent of facility failures, highlighting dynamic domino-type behaviors in complex systems [16]. Similarly, analyses of cascading scenarios in Natech risk assessment emphasize that densely packed installations such as tank farms and port facilities are especially vulnerable to domino effects due to short inter-unit distances and overlapping consequence footprints; these features can markedly amplify overall risk outcomes even when the initial triggering hazard is moderate [18,19]. These findings underscore that the spatial arrangement of storage tanks can be as influential as the intrinsic hazard of the stored substances.

In this study, a framework is developed that combines seismic hazard estimates, which are expressed in terms of peak ground acceleration, with a damage probability matrix for storage tanks in marine ports. Release footprints are then simulated and subsequently intersected with high-resolution demographic data to quantify potential exposure. Community risk is conceptualized as the expected number of individuals exposed to hazardous releases triggered by earthquake-induced damage to energy infrastructure. Critical shaking thresholds at which risk escalates sharply are identified, thereby highlighting conditions under which targeted mitigation and emergency-planning interventions would yield the greatest benefits.

The methodology is demonstrated using a case study of a typical port located on the Saint-Laurence River in the province of Quebec, Canada, located in a region of moderate seismicity in Eastern Canada, and offers the detailed data necessary to calibrate our seismic hazard, structural fragility and consequence models. The port covers approximately 12 square kilometers, bordering a metropolitan population, and contains 49 storage tanks that vary in shape and capacity.

In the present study, site-specific peak ground acceleration values were calculated for a set of earthquake scenarios with magnitudes ranging from 6.0 to 7.0 and epicentral distances between 5 km and 100 km. Fragility analysis is conducted using damage probability matrices calibrated to observed tank performance in moderate-to-strong earthquakes and is applied to derive Hazardous Release Likelihood Index (HRLi) scores at the tank scale, accounting for anchorage condition, geometry and local ground motion amplification.

Established consequence-analysis software is then employed to calculate the Maximum Distance of Effect (MDE) for releases of naphtha, LPG and methane. Finally, these effect zones on block-level population data were overlayed to derive the NRI as a continuous function of PGA.

2. Materials and Methods

This study implements a comprehensive seismic risk assessment for storage tanks, which was inspired by the Natech risk framework of Cruz and Okada [14], while enriching it with an improved scoring method for population density and cascading effects due to tanks' proximity to site-specific geospatial, structural and demographic data. The methodology enables rapid evaluation of Natech risk by linking hazard identification, vulnerability analysis and risk index calculation (Figure 1). The methodology involves several steps, including seismic hazard characterization, inventory development, damage probability assessment and estimation of HRLi scores. As illustrated in Figure 1, the inventory and damage assessment steps are supported by a schematic representation of a representative aboveground atmospheric steel storage tank, highlighting the main geometric parameters (diameter D and height H) used to estimate storage volumes and characterize tank vulnerability. Finally, an NRI is calculated for each storage tank containing hazardous substances, enabling the identification of areas within the port where seismic Natech risk is highest.

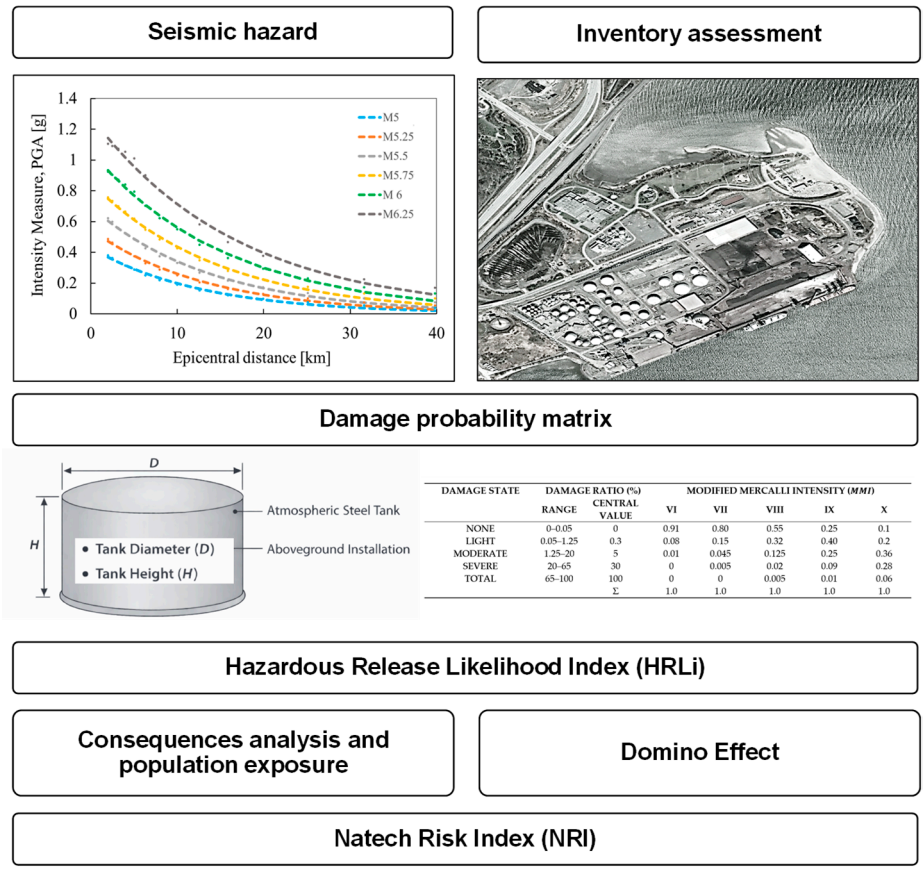

Figure 1. Framework for Natech risk assessment of storage tanks in port facilities.

This section describes the seismic Natech risk assessment methodology adopted in this study. The procedure integrates seismic hazard characterization, inventory development, damage-based hazardous release likelihood estimation, off-site consequence analysis, population exposure assessment and domino-effect modeling.

2.1. Seismic Hazard Modeling

For the seismic hazard modeling in this study, the Ground Motion Prediction Equations (GMPE) equations of Atkinson and Adams [7] are used. For each site, the epicentral distance is calculated from the earthquake location to the asset coordinates and the rock-based IM values are corrected for local site effects using amplitude and frequency-dependent site amplification factors derived from the average shear wave Vs_{30}, in accordance with the Canadian Highway Bridge Design Code (CAN/CSA S6-14 [17]).

The seismic hazard modeling in this study is based on the GMPEs developed by Atkinson and Adams [7] for Eastern Canada. These GMPEs are originally provided as discrete lookup-table values for a reference site condition corresponding to $V_{s30} = 760$ m/s (B/C boundary) and form the basis of the Canadian National Seismic Hazard Model and the seismic design input adopted in the Canadian Highway Bridge Design Code [17]. To enable direct computation of PGA as a function of earthquake magnitude and source-to-site distance, the lookup-table values were converted into a closed-form regression model following the methodology proposed by Abo El Ezz et al. [20].

Local site effects were represented using Site Class C, consistent with the recommendations of CAN/CSA S6-14 [17], to provide a code-based and uniform representation of soil conditions for screening purposes. No sensitivity analysis with respect to alternative site classes or amplification uncertainty was performed.

Alternatively, in this study, median PGA values derived from the selected GMPE are propagated through the Natech risk framework. The analysis does not incorporate lower- or upper-bound ground-motion variability or probabilistic logic-tree formulations, as the objective is to develop a deterministic, scenario-based screening methodology suitable for comparative assessment of Natech risk.

This formulation covers median, lower-bound and upper-bound PGA predictions for Eastern Canada for M_w ranging from 5.0 to 7.25 and epicentral distances up to 40 km. In the present study, only median PGA values are considered.

Rather than reproducing detailed closed-form regression equations, the median PGA is expressed here in a generalized form as follows:

$$PGA_{median} = f(M_w; R_{epi}) \quad (1)$$

where M_w is the earthquake moment magnitude (dimensionless), R_{epi} is the epicentral distance (km) and f(·) denotes the regional GMPE calibrated for Eastern Canada.

The regression reformulation adopted in this study follows the methodology described by Abo El Ezz et al. [20], which provides explicit polynomial expressions for median PGA in Eastern Canada derived from the Atkinson and Adams [7] tables.

Information regarding the exact number of tanks, their structural types and the substances stored in each unit are not publicly available. To overcome this limitation, geospatial data from Google Earth Pro were used to identify and measure the tanks, which allowed the determination of their number, dimensions and general configuration.

Moreover, in the current study, twelve (12) earthquake scenarios' combined moment magnitudes $M_w \in \{5.5; 6.0; 6.5; 7.0\}$ and epicentral distances $R_{epi} \in \{10, 20, 30\}$ km (Table 1) are compiled for the assessment of seismic risk.

The selected magnitude and distance ranges are consistent with historical seismicity and regional hazard assessments for Eastern Canada and represent near-field to intermediate-field source conditions relevant to the Saint Lawrence River corridor. The scenarios are intended as a representative, screening-level set, rather than as a probabilistic hazard model, enabling systematic evaluation of intensity-dependent Natech risk and identification of critical PGA thresholds.

Table 1. Adopted earthquake scenarios and *PGA* values.

Scenario	M_w	R_{epi}(km)	*PGA*(g)
1	5.5	10	0.20
2	6.0	10	0.30
3	6.5	10	0.48
4	7.0	10	0.80
5	5.5	20	0.10
6	6.0	20	0.17
7	6.5	20	0.28
8	7.0	20	0.41
9	5.5	30	0.05
10	6.0	30	0.09
11	6.5	30	0.16
12	7.0	30	0.28

2.2. Inventory Assessment

Inventory assessment is a crucial step in the seismic risk assessment of storage tanks, as it requires identifying and characterizing all units in terms of their physical properties, stored substances and storage conditions. For the present study, an inventory of 49 tanks located at the studied port case was established using geospatial data from Google Earth Pro. Through these platforms, the tanks were visually identified; then, their external dimensions (diameter and height) were measured in order to estimate storage volumes.

Since information on the actual contents of the tanks was not publicly available, assumptions were made regarding the products stored. Three (3) representative hazardous substances were selected (naphtha, LPG and methane), which reflect common classes of flammable or toxic materials typically handled in port facilities.

All tanks were assumed to be constructed of steel, consistent with standard design practice for aboveground atmospheric storage tanks. These steps allowed us to generate a complete dataset of tank geometries, storage volumes and assumed contents (which formed the basis for the subsequent seismic risk analysis). For consistency and conservatism, storage tanks were assumed to be fully filled; the influence of partial filling or ullage conditions was not evaluated, as such operational variability was outside the scope of the present screening-level analysis.

2.3. Intensity Conversion and HLRi

For each scenario, the *PGA* was estimated at the tank sites considering site amplification factors. Since HRLi estimation requires both *PGA* and an intensity-based measure, the Modified Mercalli Intensity (*MMI*) was derived from *PGA* following the empirical relationship of [21]. Specifically, the *MMI* is computed as follows:

$$MMI = \frac{log(PGA) - 0.014}{0.3} \quad (2)$$

where *MMI* is dimensionless, *PGA* is expressed in cm/s^2, g is the gravitational acceleration (g = 9.81 m/s^2), used to convert *PGA* values originally expressed in units of g into cm/s^2.

This conversion enables the integration of PGA-based hazard scenarios into an intensity measure more directly correlated with observed structural damage. It should be noted that the PGA–MMI conversion adopted in this study follows a commonly used empirical relationship.

The obtained *MMI* values were then coupled with fragility functions to derive the HRLi for each tank and failure mode.

To further quantify the HRLi, a damage probability matrix proposed by Seligson et al. [22] is presented in Table 2 and employed and later recommended by Cruz et al. [14]. This ap-

proach assigns discrete scores to probability intervals, facilitating integration into the *NRI* framework (see Table 3). In fact, the HRLi is defined as a discrete score ranging from 1 to 5, derived from the probability of damage obtained from the damage probability matrix. Probability ranges are mapped to HRLi scores using the conversion scheme presented in Table 3. In the subsequent NRI calculation, HRLi is treated as a dimensionless index rather than a continuous probability.

Table 2. Damage probability matrix of tanks.

Damage State	Damage Ratio (%)		Modified Mercalli Intensity (*MMI*)				
	Range	Central Value	VI	VII	VIII	IX	X
None	0–0.05	0	0.91	0.80	0.55	0.25	0.1
Light	0.05–1.25	0.3	0.08	0.15	0.32	0.40	0.2
Moderate	1.25–20	5	0.01	0.045	0.125	0.25	0.36
Severe	20–65	30	0	0.005	0.02	0.09	0.28
Total	65–100	100	0	0	0.005	0.01	0.06
		Σ	1.0	1.0	1.0	1.0	1.0

Table 3. Probability-to-score conversion matrix for HRLi estimation.

Probability Range	Score
Less than 20%	1
20–40%	2
40–60%	3
60–80%	4
More than 80%	5

2.4. Consequence Analysis and Population Exposure

Once the HRLi is determined, the potential offsite consequences of each release scenario were assessed using the U.S. Environmental Protection Agency's RMP*Comp software: RMP*Comp [23]. This latter software simulates physical and toxicological hazard zones for flammable and hazardous materials. Inputs to this model included the stored substance type, estimated inventory volume, physical state and containment conditions.

RMP*Comp produced hazard footprint contours for three consequence types: (i) thermal radiation from pool fires, (ii) overpressure from vapor cloud explosions and (iii) toxic concentration thresholds for airborne releases. For each consequence category, the *MDE*, defined as the radial distance from the tank within which the threshold consequence level is exceeded, was recorded.

The present study does not consider alternative atmospheric stability classes or three-dimensional CFD-based dispersion modeling, as such analyses are outside the scope of the proposed scenario-based Natech risk screening framework.

Population exposure is estimated using a population-density-based approach, with population density expressed in inhabitants per square kilometer (inhabitants/km^2). The exposed population is calculated using the full MDE footprint, consistent with off-site consequence assessment practices.

Population density was computed as follows:

$$\text{Population Density} = \frac{\text{Total Number of Inhabitants}}{\text{Territorial Area}} \quad (3)$$

The assumed population density is equal to 5673 inhabitants/km^2. The estimated exposed population within the impact zone was obtained using the following equation:

$$\text{Estimated exposed Population} = \text{Population Density} \times Area_{sci} \quad (4)$$

where $Area_{sci}$ represents the area of the circular MDE footprint (in km^2).

The value of $Area_{sci}$ for each hazard zone is calculated using the polygon area measurement tool in Google Earth Pro. This methodology allows the estimation, for each storage tank, of the number of individuals potentially exposed in the event of hazardous-material release.

In this study, population exposure was estimated using a spatially averaged population density derived from dissemination-block census data for the surrounding urban area. Individual block-level population counts were not explicitly overlaid in the GIS analysis, as the objective was to provide a screening-level estimate of community exposure suitable for scenario comparison rather than a parcel-scale evacuation analysis.

Based on these population estimates, an $Area_{sci}$ score was assigned as follows:

- Score 1: 1–100 inhabitants;
- Score 2: 100–500 inhabitants;
- Score 3: 500–1000 inhabitants;
- Score 4: 1000–1500 inhabitants;
- Score 5: more than 1500 inhabitants.

2.5. Domino Effect and Mean Natech Risk Index

To account for the possibility of cascading accidents, a domino effect score $D_{i,s}$ was assigned to each tank. The principle is that when a hazardous release occurs, secondary accidents may be triggered in nearby tanks if they are located within the impact zone of the initial event. In this study, the impact zone was defined as a circular buffer with a radius equal to one-third of the Maximum Distance of effect MDE, consistent with recommendations in Cruz et al. [14].

Figure 2 illustrates the procedure used to assign domino effect scores ($D_{i,s}$) to storage tanks. The scoring is based on the number of neighboring tanks located within one-third of the MDE, which defines the critical zone for cascading accident potential.

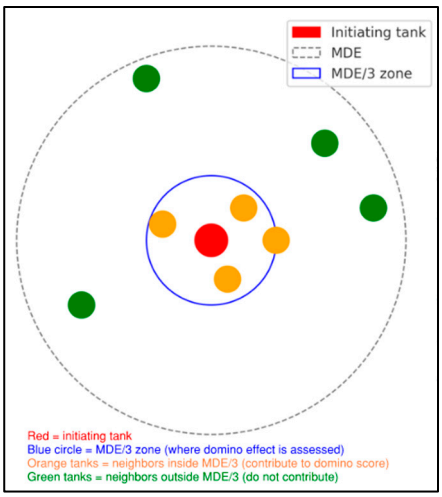

Figure 2. Illustration of the domino effect scoring method ($D_{i,s}$) applied to storage tanks.

The following scoring method was followed:

- Score 1: 1–5 tanks.
- Score 2: 6–10 tanks.
- Score 3: 11–15 tanks.
- Score 4: 16–20 tanks.
- Score 5: more than 20 tanks.

As a result, the domino effect becomes a critical amplifying factor in overall Natech risk estimation. The $NRI_{i,s}$ for each individual tank and seismic scenario was computed as follows:

$$NRI_{i,s} = HRL_{i,s} \times \left(D_{i,s} + Area_{sci_{i,s}} \right) \quad (5)$$

where i denotes the tank and s the seismic scenario.

For each scenario s, the scenario-level mean NRI is obtained by averaging over the N_t tanks in the port:

$$\overline{NRI_s} = \frac{1}{N_t} \sum_{i=1}^{N_t} (NRI_{i,s}) \quad (6)$$

It should be noted that the arithmetic mean is used to represent the average port-level Natech risk, which is conditional on a given seismic scenario, consistent with the scenario-based objective of the proposed framework.

By examining the variation in $\overline{NRI_s}$ across the full range of modeled PGAs for median GMPE predictions, it is possible to identify critical intensity thresholds where the Natech risk escalates rapidly, guiding both mitigation prioritization and emergency preparedness planning.

It is acknowledged that different accident phenomena, such as pool-fire thermal radiation, BLEVE fireballs and vapor-cloud explosions, are governed by distinct physical damage mechanisms and threshold criteria, including heat-flux intensity, blast overpressure and impulse. Standard consequence-analysis references provide dedicated physical models for each phenomenon and clearly demonstrate that escalation potential strongly depends on the nature of the initiating event and the corresponding impact metrics [24]. Quantitative studies on domino effects further show that blast overpressure and thermal radiation can propagate damage to adjacent equipment when separation distances fall within critical impact zones, significantly increasing the likelihood of cascading failures [25,26].

Implementing consequence-specific interaction radii would therefore require explicit coupling between off-site consequence modeling outputs and structural vulnerability thresholds for neighboring tanks, which is beyond the scope of the present scenario-based framework. Accordingly, the adopted MDE/3 radius should be interpreted as a conservative, generalized interaction zone and the resulting domino scores $D_{(i,s)}$ represent relative escalation potential rather than precise physical damage probabilities.

3. Results

Table 4 summarizes the values of $\overline{D_{i,s}}$ and $\overline{Area_{sci}}$ for the three substances and all scenarios. Table 5 lists the adopted seismic scenarios, including earthquake magnitude, epicentral distance, PGA, MMI and the corresponding mean $\overline{NRI_s}$ values for the three studied substances, obtained by averaging tank-level values for all 49 tanks. The scenario risk assessments are conducted assuming the same type of substance for all 49 tanks. The analyses are then presented for each type of substance separately.

To illustrate how the $\overline{NRI_s}$ values in Table 5 were obtained, this subsection presents a complete intermediate calculation for Naphta's $\overline{NRI_s}$ value for the Scenario 6, corresponding to $M_w = 6.0$ and $R_{epi} = 20$ km.

First, the PGA at the tank site is estimated using the regional GMPE of Atkinson and Adams [17]. For this magnitude–distance pair, the resulting ground motion is PGA = 0.17 g.

Next, the $HRL_{i,s}$ is obtained by combining the intensity level with the damage-probability matrix of Seligson et al. [22]. For a welded atmospheric tank subjected to MMI = VII, the expected mean value of $HRL_{i,s} = 0.15$ (score = 1) (see Table 3).

The domino effect score is then assigned using the approach of Cruz and Okada [14]. A circular buffer with a radius equal to one-third of MDE is drawn around each tank.

The number of neighboring tanks within this buffer is counted. For this scenario, a mean domino score $\overline{D_{i,s}} = 4.95$ for 49 tanks is adopted, which represents a very low escalation potential (see Table 4).

Table 4. Mean $\overline{D_{i,s}}$ and $\overline{Area_{sci}}$ estimations for all substances and scenarios.

Substance	Scenario	$\overline{D_{i,s}}$	$\overline{Area_{sci}}$
Naphta	1	4.96	5
	2	4.95	5
	3	5	5
	4	5	5
	5	5	4.61
	6	5	4.61
	7	5	5
	8	5	4.61
	9	5	5
	10	5	5
	11	3	5
	12	3	5
LPG	1	3.33	2.33
	2	3.33	2.28
	3	3.33	2.33
	4	3.33	2.31
	5	3.33	2.31
	6	3.33	2.31
	7	3.33	2.31
	8	3.33	1.73
	9	3.33	2.31
	10	3.33	2.31
	11	3.33	2.31
	12	3.33	2.31
Methane	1	2	1.73
	2	2	1.73
	3	2	1.73
	4	2	1.73
	5	2	1.73
	6	2	1.73
	7	2	1.73
	8	2	1.73
	9	2	1.73
	10	2	1.73
	11	2	1.73
	12	2	1.73

Population exposure is then assessed by combining hazard footprint contours from RMP*Comp with local demographic data. For scenario 6, the estimated number of exposed individuals is approximately 15,480 inhabitants, corresponding to a mean exposure score $\overline{Area_{sci}} = 5$ for all 49 tanks (see Table 4).

Table 4 reports scenario-averaged values of $\overline{D_{i,s}}$ and $\overline{Area_{sci}}$ obtained by averaging tank-level scores over all storage tanks.

This value represents the tank-level index $NRI_{i,6}$ for a given naphtha tank under Scenario 6. In practice, $NRI_{i,6}$ is computed for each of the 49 tanks, and the scenario-level mean index reported in Table 5 $\left(\overline{NRI_6} = 9.95\right)$ is obtained by averaging these 49 values according to Equation (6).

Table 5. Mean $\overline{NRI_s}$ estimation for all scenarios.

Scenario	M_w	R_{epi} (km)	*PGA* (g)	*MMI*	$HRL_{i,s}$ Probability (Score)	$\overline{NRI_s}$ Naphtha	$\overline{NRI_s}$ LPG	$\overline{NRI_s}$ Methane
1	5.5	10	0.2059	VIII	15% (1)	9.95	5.69	3.73
2	6.0	10	0.3099	VIII	15% (1)	9.95	5.69	3.73
3	6.5	10	0.4866	IX	34% (3)	19.91	11.30	7.47
4	7.0	10	0.8044	X	64% (4)	39.83	22.53	15.00
5	5.5	20	0.1049	VII	5% (1)	9.95	5.69	3.73
6	6.0	20	0.1725	VII	15% (1)	9.95	5.69	3.73
7	6.5	20	0.4192	VIII	15% (1)	9.95	5.69	3.73
8	7.0	20	0.2839	IX	24% (2)	19.91	11.3	7.47
9	5.5	30	0.0534	VI	1% (1)	9.95	5.69	3.73
10	6.0	30	0.0960	VII	5% (1)	9.95	5.69	3.73
11	6.5	30	0.1656	VII	5% (1)	9.95	5.69	3.73
12	7.0	30	0.2863	VII	5% (1)	9.95	5.69	3.73

To further explore the relationship between seismic intensity and Natech risk, Figure 3 illustrates the variation in the scenario-level mean $\overline{NRI_s}$ as a function of PGA for naphtha, LPG and methane. The plotted points represent the scenario-based results, while the dashed curves correspond to regression fits (see Equations (7)–(9) for regression fits).

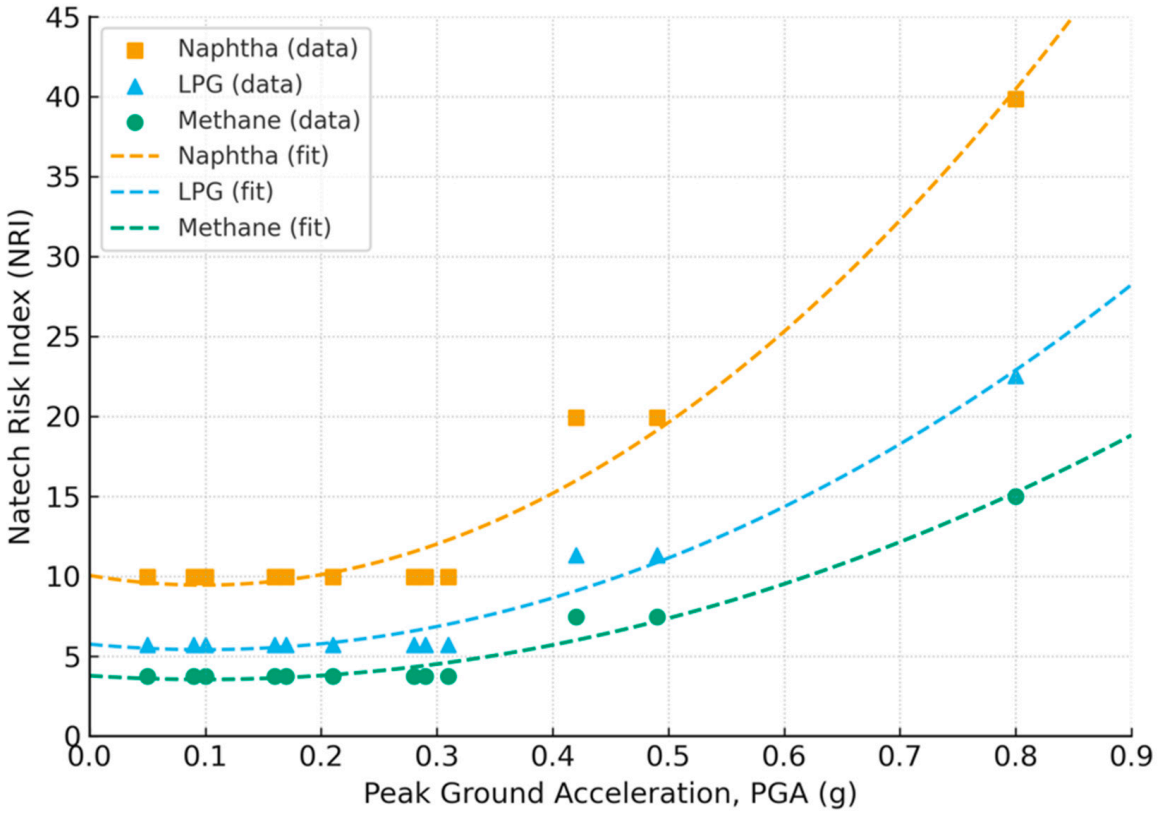

Figure 3. Variation in the $\overline{NRI_s}$ as a function of PGA for naphtha, LPG and methane (scenario-averaged over all 49 tanks and across 12 seismic scenarios).

The following equations are the regression fits of mean $\overline{NRI_s}$ in function of PGA for naphtha, LPG and methane, respectively:

$$\overline{NRI}_{Naphta} = 62.96 \cdot PGA^2 - 12.35 \cdot PGA + 10.0 \ (R^2 = 0.968) \quad (7)$$

where $\overline{NRI}_{Naphta}$ denotes the mean NRI for naphta over all tanks for a given scenario.

$$\overline{NRI}_{LPG} = 35.49 \cdot PGA^2 - 6.97 \cdot PGA + 5.74 \ (R^2 = 0.967) \quad (8)$$

where $\overline{NRI}_{LPG}$ denotes the mean NRI for LPG over all tanks for a given scenario.

$$\overline{NRI}_{Methane} = 23.81 \cdot PGA^2 - 4.72 \cdot PGA + 3.77 \ (R^2 = 0.968) \quad (9)$$

where $\overline{NRI}_{Methane}$ denotes the mean NRI for methane over all tanks for a given scenario.

The quadratic regression relationships are derived from a limited number of high-PGA scenarios and are intended to illustrate the non-linear escalation of scenario-averaged Natech risk with increasing PGA. While the fitted curves capture the overall trend, the stability of the regression coefficients in the transition region would benefit from a denser sampling of earthquake scenarios at intermediate PGA levels. These relationships should therefore be interpreted as empirical, scenario-based trend representations rather than fully predictive models.

Figure 3 highlights how risk levels escalate nonlinearly with increasing PGA, particularly for naphtha, which exhibits higher sensitivity compared to LPG and methane. The regression curves are empirical, scenario-based fits illustrating non-linear risk escalation; additional earthquake scenarios would further refine coefficient stability in the transition region.

In addition, points represent scenario-averaged NRI values obtained by averaging across all tanks, as the figure focuses on inter-scenario risk escalation trends at the port scale.

4. Discussion

Based on Table 5., results of the NRI assessment across the twelve (12) seismic scenarios demonstrate that both the level of ground motion and the nature of the stored substances play critical roles in determining overall risk. A first observation is that moderate seismic scenarios (Scenarios 1, 2, 5, 6, 7, 9, 10, 11 and 12), corresponding to PGA values below 0.3 g and MMI of VII–VIII, generally yield stable and moderate $\overline{NRI_s}$ values. This behavior is consistent with recent scenario-based seismic Natech studies, which emphasize that risk escalation becomes pronounced after critical shaking thresholds because release likelihood increases non-linearly once damage states transition from light/moderate to severe. For example, Shafiei-Moghaddam et al. [3] used multiple earthquake hazard scenarios to assess chemical release risk and demonstrated how estimated risk levels vary strongly with scenario intensity. Similarly, Amaducci et al. [27] developed a quantitative risk assessment framework for earthquake-triggered Natech scenarios in pipeline systems, showing the relevance of integrated intensity–risk relationships for seismic risk management.

In these cases, naphtha consistently emerges as the most hazardous substances, with $\overline{NRI_s}$ scores close to 10, while LPG and methane remain in the lower-risk range.

The stability of NRI across different magnitudes but similar intensity classes (e.g., Scenarios 1 vs. 2, or Scenarios 5 vs. 6) highlights the dominant influence of MMI over earthquake magnitude alone in driving release probabilities and risk escalation.

In contrast, higher-intensity scenarios (Scenarios 3, 4 and 8), characterized by PGA values of 0.49 g and above and MMI levels of IX, show a sharp increase in $\overline{NRI_s}$ values.

Under these conditions, naphtha exhibits significantly higher risk values, reflecting their high volatility, flammability and potential to generate widespread impacts in the event of structural failure.

LPG also transitions from a low-to-moderate risk category (mean $\overline{NRI_s} \approx 11.3$–$22.5$), while methane, although still the lowest among the four, reaches values (mean $\overline{NRI_s} \approx 15$) that should not be overlooked. These findings indicate a nonlinear escalation of Natech

risk once seismic intensity surpasses the VIII–IX threshold, consistent with fragility-based expectations of severe structural damage and increased release likelihood.

Another important finding is the role of tank clustering within the port. The short distances observed between several storage units substantially increase the probability of cascading accidents, meaning that even moderate release scenarios could lead to chain reactions involving multiple tanks. This configuration magnifies population exposure, particularly for naphtha tanks located near residential areas. Consequently, the proximity of tanks and their interaction through domino effects is as critical as the intrinsic hazard of the stored substances.

To quantify clustering, the inter-tank distances were measured by geospatial analysis. Table 6 summarizes representative distances between selected tanks across the port.

Table 6. Distances between representative tanks in the studied port.

Tanks	Distance (m)	Tanks	Distance (m)	Tanks	Distance (m)
1–2	35.14	16–18	25.86	32–34	24.03
1–3	32.71	17–19	21.17	33–34	32.25
2–4	52.30	18–19	31.61	33–35	20.80
3–4	40.18	17–20	29.18	34–36	17.58
3–5	25.70	19–21	35.62	35–36	18.77
4–5	45.34	20–21	16.45	37–38	187.03
5–6	24.50	21–22	19.74	37–16	124.84
6–7	36.74	22–23	25.17	39–40	11.07
6–8	37.53	23–28	20.62	40–42	9.39
8–9	42.92	20–23	44.37	39–41	9.50
7–9	31.69	23–28	19.77	41–42	10.71
7–10	53.20	23–32	28.61	41–43	12.28
9–10	71.33	18–24	33.57	41–44	12.23
10–11	82.99	24–25	25.19	42–44	16.00
10–12	81.78	25–26	21.10	42–45	11.88
12–14	50.69	26–27	35.91	43–44	9.91
11–12	45.42	28–29	14.22	44–45	8.10
11–14	37.61	28–32	14.62	46–47	9.26
12–13	41.38	29–30	14.53	46–49	8.12
13–14	50.16	29–31	18.38	47–48	7.51
13–15	24.01	30–31	20.72		
14–15	44.40	31–32	18.66		
16–17	16.88	31–33	51.32		

The results highlight several critical proximities well below 20 m, with some pairs separated by less than 10 m (e.g., tanks 44–45 at 8.1 m, tanks 47–48 at 7.5 m, tanks 41–42 at 10.7 m). These minimal separations fall within typical thermal radiation and overpressure footprints, confirming that the likelihood of cascading Natech events is high in the studied port.

These findings are consistent with a broad body of the Natech risk literature emphasizing the dominant influence of spatial configuration and inter-unit distances on escalation potential. Early foundational work by Cruz and Okada [14] demonstrated that closely spaced storage tanks substantially increase the likelihood of domino effects under both seismic and thermal loading, particularly when separation distances fall within characteristic thermal radiation or overpressure impact zones. Similarly, Necci et al. [28] showed that insufficient inter-tank spacing is one of the primary drivers of cascading accidents in Natech scenarios, often outweighing the contribution of the initial triggering hazard.

On the other hand, Figure 3 (see above) highlights several key observations, which are summarized as follows:

- For naphtha, a low-to-moderate risk is observed for PGA values greater than or equal to 0.31 g with mean $\overline{NRI_s} \approx 10$, followed by a significant to critical risk when PGA reaches or exceeds 0.42 g with $\overline{NRI_s} \approx 20$ and finally a catastrophic risk at $PGA = 0.8$ g with mean $\overline{NRI_s} \approx 40$. These products are highly flammable and in the event of rupture or leakage, they present a high risk of fire or explosion.
- For LPG, the risk remains low for $PGA \leq 0.31$ g with $\overline{NRI_s} \approx 5.69$, becomes significant at $PGA \geq 0.42$ g with mean $\overline{NRI_s} \approx 11.30$ and reaches a critical level at PGA = 0.8 g with mean $\overline{NRI_s} \approx 22.53$. In the event of a gaseous release, the consequences include a high risk of boiling liquid expanding vapor explosion and possible domino effects.
- For methane gas, the risk is low for $PGA \leq 0.31$ g with mean $\overline{NRI_s} \approx 3.73$, becomes moderate to significant at $PGA \geq 0.42$ g and finally reaches a critical level at $PGA = 0.8$ g with mean $\overline{NRI_s} \approx 15.00$. Methane is highly flammable and poses a significant risk of explosion.

The curves reveal three distinct phases: a nearly linear phase for PGA < 0.3 g, a critical transition phase for 0.3 g < PGA < 0.5 g and a nonlinear escalation for PGA > 0.5 g. As PGA increases, the mean $\overline{NRI_s}$ consistently rises for all products, with naphtha showing the highest sensitivity and the largest $\overline{NRI_s}$ values. LPG and methane also show increasing risk, but their mean $\overline{NRI_s}$ values remain lower for the same PGA. Data analysis shows that seismic risk increases sharply when PGA exceeds about 0.4 g. At this threshold, damage to energy infrastructures becomes much more severe, as confirmed in Scenarios 3, 4 and 8, where PGA $\geq$ 0.42 g. In these cases, the risk index for storage tanks reaches critical or even catastrophic levels, up to mean $\overline{NRI_s} \approx 40$.

Overall, the analysis highlights that naphtha represents the dominant contributor to Natech risk at the studied port, especially under high-intensity seismic shaking. LPG and methane, while comparatively less hazardous in moderate scenarios, still pose significant risks under strong ground motions due to their physical properties and storage conditions. These results underscore the importance of differentiated risk management strategies: reinforcing safety and containment measures for naphtha tanks, while ensuring adequate monitoring and contingency planning for LPG and methane installations.

Finally, the regression relationships between the mean Natech Risk Index $\overline{NRI_s}$ and PGA provide insight into how seismic Natech risk evolves as ground-motion intensity increases. The results indicate the existence of seismic intensity thresholds beyond which risk escalates nonlinearly, reflecting the transition from limited damage to widespread structural failure and cascading effects. This behavior is consistent with the established Natech literature, which shows that accident escalation becomes dominant once severe damage states are reached and domino mechanisms are activated in clustered industrial facilities. Krausmann et al. [29] highlighted the critical role of spatial configuration and escalation effects in governing Natech consequences and emphasized that scenario-based approaches are particularly well suited for capturing such nonlinear behaviors in complex industrial systems. In addition, official guidance by Necci and Krausmann [28] stresses that Natech risk assessment tools should be transparent, reproducible and operational, especially in contexts where detailed facility data or fully probabilistic analyses are not feasible. Within this broader context, the proposed framework contributes a practical, scenario-based workflow that links seismic hazard intensity, release likelihood, off-site consequences, population exposure and escalation potential within a single screening indicator, supporting risk-informed decision-making for marine ports located in regions of moderate seismicity.

5. Conclusions

This study presented a framework to quantify seismic Natech risk in a representative port on the Saint-Laurence River in Quebec. By integrating regional seismic hazard estimates, damage-based Hazardous Release Likelihood Index HRLi scores, offsite consequence modeling and demographic exposure, the approach captures the full pathway from earthquake shaking to community-level impacts.

Results indicate that Natech risk remains moderate under shaking intensities of $PGA \leq 0.3$ g (MMI = VII–VIII) but escalates sharply once PGA exceeds 0.4 g (MMI = X). Naphtha was identified as the dominant risk drivers, with NRI values reaching catastrophic levels ($\overline{NRI_s} \approx 40$ at $PGA = 0.8$ g), while LPG and methane also showed significant escalation, including the potential for boiling liquid expanding vapor explosions. These findings underline the critical need for targeted risk reduction measures at marine ports located in regions of moderate seismicity.

A key outcome of this study is the establishment of regression relationships between NRI and PGA, which capture the nonlinear escalation of Natech risk with increasing seismic intensity. Notably, these equations can provide a quantitative foundation for future mitigation solutions, enabling researchers to predict how interventions such as anchorage retrofitting or soil densification may shift the risk curves and reduce vulnerabilities.

An important finding of this work is the critical role of tank clustering. The short distances observed between many tanks (often less than 20 m and in some cases below 10 m (e.g., tanks 44–45 separated by only 8.1 m, tanks 47–48 by 7.5 m and tanks 40–42 by 9.4 m)) significantly increase the probability of cascading accidents.

Under seismic-induced release, this proximity makes it highly likely that domino effects would trigger multiple tank failures, magnifying exposure for nearby communities. For example, clusters of naphtha tanks located near residential zones present particularly severe risks, as simultaneous releases could generate overlapping hazard zones. This configuration indicates that proximity and interaction between tanks are as critical as the intrinsic hazard of the stored substances and should therefore be explicitly integrated into site-specific Natech risk management strategies.

Overall, this proposed framework provides a tool to compare risk contributions and prioritize mitigation. Its adoption would strengthen seismic resilience in marine energy hubs while enhancing the safety of surrounding urban populations.

Future studies could refine population exposure estimates by explicitly overlaying dissemination-block population data from Statistics Canada within GIS environments, allowing tank-specific $Area_{sci}$ values to be computed. Such refinements would improve local resolution but are not expected to alter the scenario-averaged NRI trends identified in this study.

Additionally, future work should focus on expanding the set of earthquake scenarios, particularly at intermediate-to-high PGA levels, to further refine regression stability and enhance predictive robustness.

As future work, mitigation simulations could be performed to evaluate the effectiveness of various intervention strategies for reducing seismic Natech risk. Such analyses would help identify how structural and geotechnical improvements can influence tank fragility and site-wide risk indices. For example, anchorage retrofit studies such as those by Phan et al. [30] demonstrate that anchored configurations perform substantially better than unanchored tanks under seismic loading, suggesting that similar simulations could quantify how increased anchorage capacity modifies local damage probabilities. Likewise, geotechnical investigations on soil densification and liquefaction resistance [31–33] provide a foundation for modeling how improvements in subgrade stiffness (e.g., higher Vs_{30} values) might mitigate foundation instability and reduce overall risk. Incorporating these

types of mitigation scenarios into future numerical simulations would extend the present framework beyond risk quantification toward the development of actionable resilience and retrofit strategies for coastal ports. Additionally, probabilistic seismic reliability frameworks similar to those developed by Nassar et al. [34–36] for bridges could be extended to industrial port facilities for evaluating how mitigation measures (e.g., anchorage enhancement, base-isolation strategies and foundation improvement) influence overall Natech risk. Adapting such methodologies to storage-tank systems would allow for future research on designing resilience strategies for coastal ports.

Additionally, future extensions of the proposed framework could refine the domino-effect modeling by introducing consequence-specific interaction radii based on physical damage thresholds, such as thermal radiation levels for pool fires, overpressure criteria for vapor-cloud explosions or fireball radiation for BLEVE events. Incorporating heat-flux- or overpressure-based interaction distances would allow a more detailed representation of cascading failure mechanisms and could lead to substance- and release-type-dependent modifications of the domino-effect scores $D_{i,s}$.

While such refinements would increase model complexity and data requirements, they represent a natural progression toward higher-fidelity Natech risk assessments for port facilities, particularly when detailed consequence modeling and structural vulnerability data are available.

Limitations and Assumptions

The proposed seismic Natech risk assessment framework is intended as a screening-level, scenario-based methodology and several simplifying assumptions were adopted to ensure applicability in data-limited contexts. All storage tanks are assumed to be aboveground atmospheric steel tanks, consistent with common practice for large fuel and chemical storage facilities in marine ports. Detailed information on tank construction, anchorage systems, shell thickness and retrofitting history was not publicly available and therefore could not be explicitly modeled. While these factors influence seismic performance, their omission is consistent with the objective of comparative risk screening rather than detailed structural assessment.

Tank geometries and storage volumes were estimated using geospatial measurements from satellite imagery, which introduces uncertainty related to measurement resolution and the absence of detailed design drawings. The assumed tank characteristics are applied uniformly across scenarios to isolate the influence of seismic intensity, consequence magnitude and spatial configuration on Natech risk.

Consequently, the reported NRI values should be interpreted as relative indicators of risk escalation rather than absolute predictions of damage or release probability. These assumptions do not affect the identification of critical PGA thresholds but may influence the absolute magnitude of risk indices. Future studies could refine the analysis by incorporating tank-specific design and geotechnical data where available.

Author Contributions: M.N.: Methodology, result illustration, writing: original draft. F.M.: Methodology, formal analysis, writing: review and editing. A.A.E.E.: Conceptualization, methodology, supervision, writing: review and editing. All authors have read and agreed to the published version of the manuscript.

Funding: This study was supported through funding by École de Technologie Supérieure.

Data Availability Statement: All data generated or analyzed during this study are included in this article.

Conflicts of Interest: The authors declare no conflicts of interest.

Abbreviations

The following abbreviations are used in this manuscript:

NRI	Natech Risk Index
$NRI_{i,s}$	Natech Risk Index for tank i under seismic scenario s
$\overline{NRI_s}$	Mean Natech Risk Index for all tanks under seismic scenario s
PGA	Peak Ground Acceleration
GMPE	Ground Motion Prediction Equations
HRLi	Hazardous Release Likelihood Index
MDE	Maximum Distance of Effect
BLEVE	Boiling Liquid Expanding Vapor Explosion
CFD	Computational Fluid Dynamics
IM	Intensity Measure
LPG	Liquefied Petroleum Gas
MMI	Modified Mercalli Intensity
M_w	Moment Magnitude
R_{epi}	Epicentral Distance
V_{s30}	Average shear-wave velocity in the upper 30 m of soil

References

1. Cruz, A.M.; Krausmann, E. Vulnerability of the oil and gas sector to climate change and extreme weather events. *Clim. Change* **2013**, *121*, 41–53. [CrossRef]
2. Huang, Z.-K.; Zeng, N.-C.; Zhang, D.-M.; Argyroudis, S.; Mitoulis, S.-A. Resilience Models for Tunnels Recovery After Earthquakes. *Engineering* **2025**, *54*, 320–345. [CrossRef]
3. Shafiei-Moghaddam, P.; Jahangiri, K.; Hassani, N. Chemical release risk assessment in earthquake: Natech event scenario. *Heliyon* **2024**, *10*, e28797. [CrossRef]
4. Kabir, G.; Suda, H.; Cruz, A.M.; Giraldo, F.M.; Tesfamariam, S. Earthquake-related Natech risk assessment using a Bayesian belief network model. *Struct. Infrastruct. Eng.* **2019**, *15*, 725–739. [CrossRef]
5. Yazici, G.; Cili, F. Evaluation of the liquid storage tank failures in the 1999 Kocaeli Earthquake. In Proceedings of the 14th World Conference on Earthquake Engineering, Beijing, China, 12–17 October 2008.
6. Fabbrocino, G.; Iervolino, I.; Orlando, F.; Salzano, E. Quantitative risk analysis of oil storage facilities in seismic areas. *J. Hazard. Mater.* **2005**, *123*, 61–69. [CrossRef]
7. Atkinson, G.M.; Adams, J. Ground motion prediction equations for application to the 2015 Canadian national seismic hazard maps. *Can. J. Civ. Eng.* **2013**, *40*, 988–998. [CrossRef]
8. Pezeshk, S.; Zandieh, A.; Tavakoli, B. Hybrid empirical ground-motion prediction equations for eastern North America using NGA models and updated seismological parameters. *Bull. Seismol. Soc. Am.* **2011**, *101*, 1859–1870. [CrossRef]
9. Pavel, F.; Vacareanu, R.; Cioflan, C.; Iancovici, M. Spectral characteristics of strong ground motions from intermediate-depth Vrancea seismic source. *Bull. Seismol. Soc. Am.* **2014**, *104*, 2842–2850. [CrossRef]
10. Valente, M.; Ricci, F.; Cozzani, V. A systematic review of Resilience Engineering applications to Natech accidents in the chemical and process industry. *Reliab. Eng. Syst. Saf.* **2025**, *255*, 110670. [CrossRef]
11. Rodriguez, D.J.C.; Barresi, A.A.; Demichela, M. Critical infrastructure multi-risk deployment: An innovative framework to support NaTech preparedness in industrial facilities. *Process Saf. Environ. Prot.* **2025**, *202*, 107736. [CrossRef]
12. Lamontagne, M.; Halchuk, S.; Cassidy, J.F.; Rogers, G.C. *Significant Canadian Earthquakes 1600–2017*; Geological Survey of Canada: Ottawa, ON, Canada, 2018.
13. Franco, S.I.; Canet, C.; Iglesias, A.; González, C.V. Seismic activity in the Gulf of Mexico. A preliminary analysis. *Boletín Soc. Geol. Mex.* **2013**, *65*, 447–455. [CrossRef]
14. Cruz, A.M.; Okada, N. Methodology for preliminary assessment of Natech risk in urban areas. *Nat. Hazards* **2008**, *46*, 199–220. [CrossRef]
15. Showalter, P.S.; Myers, M.F. Natural Disasters in the United States as Release Agents of Oil, Chemicals, or Radiological Materials Between 1980–1989: Analysis and Recommendations. *Risk Anal.* **1994**, *14*, 169–182. [CrossRef]
16. Zhou, L.; Chen, G.; Zheng, M.; Gao, X.; Luo, C.; Rao, X. Agent-based modeling methodology and temporal simulation for Natech events in chemical clusters. *Reliab. Eng. Syst. Saf.* **2024**, *243*, 109888. [CrossRef]
17. *CAN/CSA-S6-14*; Canadian Highway Bridge Design Code. CSA Group: Mississauga, ON, Canada, 2014.

18. Ricci, F.; Yang, M.; Reniers, G.; Cozzani, V. Emergency response in cascading scenarios triggered by natural events. *Reliab. Eng. Syst. Saf.* **2024**, *243*, 109820. [CrossRef]
19. Misuri, A.; Cozzani, V. A paradigm shift in the assessment of Natech scenarios in chemical and process facilities. *Process Saf. Environ. Prot.* **2021**, *152*, 338–351. [CrossRef]
20. Abo-El-Ezz, A.; Farzam, A.; Fezai, H.; Nollet, M.-J. Scenario-based earthquake damage assessment of highway bridge networks. *Adv. Bridge Eng.* **2023**, *4*, 3. [CrossRef]
21. Abo-El-Ezz, A.; Houalard, C.; Nollet, M.-J.; Assi, R. Vulnerability assessment of seismic induced out-of-plane failure of unreinforced masonry wall buildings. *Can. J. Civ. Eng.* **2017**, *44*, 1045–1055. [CrossRef]
22. Seligson, H.A.; Eguchi, R.T.; Tierney, K.J.; Richmond, K. *Chemical Hazards, Mitigation and Preparedness in Areas of High Seismic Risk: A Methodology for Estimating the Risk of Post-Earthquake Hazardous Materials Release*; National Center for Earthquake Engineering Research: Taipei City, Taiwan, 1996.
23. RMP*Comp. Available online: https://cdxapps.epa.gov/olem-rmp-maintain/action/rmp-comp (accessed on 1 December 2025).
24. van den Bosch, C.J.H.; Weterings, R.A.P.M. *Methods for the Calculation of Physical Effects "Yellow Book"*; Committee for the Prevention of Disasters: The Hague, Denmark, 2005.
25. Cozzani, V.; Salzano, E. The quantitative assessment of domino effects caused by overpressure: Part I. Probit models. *J. Hazard. Mater.* **2004**, *107*, 67–80. [CrossRef]
26. Sun, D.; Jiang, J.; Zhang, M.; Wang, Z. Influence of the source size on domino effect risk caused by fragments. *J. Loss Prev. Process Ind.* **2015**, *35*, 211–223. [CrossRef]
27. Amaducci, F.; Misuri, A.; Bonvicini, S.; Salzano, E.; Cozzani, V. Quantitative risk assessment of Natech scenarios triggered by earthquakes involving pipelines. *Reliab. Eng. Syst. Saf.* **2024**, *245*, 109993. [CrossRef]
28. Necci, A.; Krausmann, E. *Natech Risk Management*; JRC Publications Repository: Brussels, Belgium, 2022; Volume 10, p. 666413.
29. Krausmann, E.; Cozzani, V.; Salzano, E.; Renni, E. Industrial accidents triggered by natural hazards: An emerging risk issue. *Nat. Hazards Earth Syst. Sci.* **2011**, *11*, 921–929. [CrossRef]
30. Phan, H.N.; Paolacci, F.; Di Filippo, R.; Bursi, O.S. Seismic vulnerability of above-ground storage tanks with unanchored support conditions for Na-tech risks based on Gaussian process regression. *Bull. Earthq. Eng.* **2020**, *18*, 6883–6906. [CrossRef]
31. Bao, X.; Jin, Z.; Cui, H.; Chen, X.; Xie, X. Soil liquefaction mitigation in geotechnical engineering: An overview of recently developed methods. *Soil Dyn. Earthq. Eng.* **2019**, *120*, 273–291. [CrossRef]
32. Bhanwar, P.; Dave, T. A review on soil liquefaction mitigation techniques and its preliminary selection. In Proceedings of the Indian Geotechnical Conference 2019: IGC-2019 Volume III, Surat, India, 19–21 December 2019; Springer: Singapore, 2019.
33. Idriss, I.M.; Boulanger, R.W. *Soil Liquefaction During Earthquakes*; Earthquake Engineering Research Institute: Oakland, CA, USA, 2008.
34. Nassar, M.; Guizani, L.; Nollet, M.J.; Tahan, A. A probabilistic approach to assess seismic base-isolated bridges reliability in cold climate. In Proceedings of the 11th National Conference in Earthquake Engineering, Los Angeles, CA, USA, 25–29 June 2018.
35. Nassar, M.; Guizani, L.; Nollet, M.-J.; Tahan, A. Seismic reliability assessment of base-isolated bridges in Quebec. *Can. J. Civ. Eng.* **2022**, *49*, 242–254. [CrossRef]
36. Nassar, M.; Guizani, L.; Nollet, M.-J.; Tahan, A. Effects of temperature, analysis and modelling uncertainties on the reliability of base-isolated bridges in Eastern Canada. *Structures* **2022**, *37*, 295–304. [CrossRef]